

Data analyses of fatigue tests by extensometry in hip prosthesis of the Co-28Cr-6Mo alloy

Análise de dados de ensaio de fadiga por Extensometria em prótese de quadril da liga Co-28Cr-6Mo

Análisis de datos de ensayos de fatiga por extensometría en prótesis de cadera de la aleación Co-28Cr-6Mo

Received: 03/09/2022 | Reviewed: 03/16/2022 | Accept: 03/17/2022 | Published: 03/25/2022

Caique Movio Pereira de Souza

ORCID: <https://orcid.org/0000-0002-3741-1036>
Universidade Presbiteriana Mackenzie, Brazil
E-mail: caiquemovio@gmail.com

Raul Gaspari Santos

ORCID: <https://orcid.org/0000-0001-7106-3752>
Universidade Estadual de Campinas, Brazil
E-mail: gaspari.raul@ifsp.edu.br

Renato Chaves Souza

ORCID: <https://orcid.org/0000-0002-8804-2752>
Instituto Federal de Educação, Ciência e Tecnologia de São Paulo, Brazil
E-mail: renatochaves@yahoo.com

Vanderlei Araujo Militão

ORCID: <https://orcid.org/0000-0002-0589-2752>
Serviço Nacional de Aprendizagem Industrial, Brazil
E-mail: vamiltao0912@gmail.com

Isaias Gouveia Silva

ORCID: <https://orcid.org/0000-0002-0789-3089>
Serviço Nacional de Aprendizagem Industrial, Brazil
E-mail: isaias.gouveia@sp.senai.br

Vanessa Seriacopi

ORCID: <https://orcid.org/0000-0002-1903-867X>
Instituto Mauá de Tecnologia, Brazil
E-mail: vanessa.seriacopi@gmail.com

Wilson Carlos da Silva Junior

ORCID: <https://orcid.org/0000-0001-8128-281X>
Instituto Federal de Educação, Ciência e Tecnologia de São Paulo, Brazil
E-mail: wilsoncarlos@ifsp.edu.br

Abstract

ANVISA made changes to its regulations, setting new values for the fatigue tests, increasing the number of cycles that prostheses must endure without presenting failures. The standard used is ABNT NBR 7206-6:2013, in which all prostheses being commercialized must be tested in the new parameters. In this article, studies were conducted based on the requirement to revalidate the Co-26Cr-6Mo metallic alloy (ASTM F75). Microstructural characterizations (Optical and Scanning Electron Microscopies), and fatigue tests were carried out, with the aim of obtaining the mechanical behavior and features of the materials used in hip prostheses and comparing them with the standard. The grain size and inclusion contents were found to be controlled. Likewise, the prosthesis has with stand 10,000,000 cycles, and has not shown cracks, nor plastic deformations, enabling the biomedical use of this alloy according to the new regulations. Tensile test and liquid penetrant inspection were also carried out to take the parameters of the related physical properties. In the analysis with strain gauges, it was possible to detect the purely elastic deformation that occurred with the application of the load during fatigue tests, resulting in a slight variation of stress in the data acquisition system.

Keywords: Hip Prosthesis; ASTM F75; Fatigue Test; Extensometry; ABNT NBR 7206-6:2013 standard.

Resumo

A ANVISA realizou alterações em sua regulamentação, estabelecendo novos valores para os ensaios de fadiga, aumentando o número de ciclos que as próteses devem suportar sem apresentar falhas. A norma utilizada é a ABNT NBR 7206-6:2013, na qual todas as próteses que estão sendo comercializadas devem ser testadas nos novos

parâmetros. Neste artigo, foram realizados estudos com base na exigência de revalidação da liga metálica Co-26Cr-6Mo (ASTM F75). Foram realizadas caracterizações microestruturais (Microscopias Óptica e Eletrônica de Varredura) e ensaios de fadiga, com o objetivo de obter o comportamento mecânico e as características dos materiais utilizados nas próteses de quadril e compare-los com a norma. O tamanho de grão e os teores de inclusão foram controlados. Da mesma forma, as próteses resistiram a 10.000.000 de ciclos, e não apresentando trincas, nem deformações plásticas, possibilitando o uso biomédico desta liga de acordo com as novas regulamentações. Os ensaios de tração e o ensaio de líquido penetrante também foram realizados para obtenção dos parâmetros das propriedades físicas relacionadas. Na análise com extensômetros foi possível detectar a deformação puramente elástica que ocorreu com a aplicação da carga durante os ensaios de fadiga, resultando em uma pequena variação de tensão no sistema de aquisição de dados.

Palavras-chave: Próteses de Quadril; ASTM F75; Ensaio de Fadiga; Extensometria; ABNT NBR 7206-6:2013.

Resumen

ANVISA realizó modificaciones en su normativa, fijando nuevos valores para las pruebas de fatiga, aumentando el número de ciclos que las prótesis deben soportar sin presentar fallas. La norma utilizada es la ABNT NBR 7206-6:2013, en la que todas las prótesis que se comercializan deben ser probadas en los nuevos parámetros. En este artículo se realizaron estudios en base al requisito de revalidar la aleación metálica Co-26Cr-6Mo (ASTM F75). Se realizaron caracterizaciones microestructurales (Microscopía Óptica y Electrónica de Barrido), y ensayos de fatiga, con el objetivo de obtener el comportamiento mecánico y las características de los materiales utilizados en las prótesis de cadera y compararlos con el estándar. Se encontró que el tamaño de grano y los contenidos de inclusión estaban controlados. Asimismo, la prótesis ha resistido 10.000.000 de ciclos, y no ha presentado grietas, ni deformaciones plásticas, lo que permite el uso biomédico de esta aleación de acuerdo con la nueva normativa. También se realizaron pruebas de tracción e inspección por líquidos penetrantes para tomar los parámetros de las propiedades físicas relacionadas. En el análisis con galgas extensiométricas se pudo detectar la deformación puramente elástica que se presentaba con la aplicación de la carga durante los ensayos de fatiga, resultando en una ligera variación de esfuerzos en el sistema de adquisición de datos.

Palabras clave: Prótesis de Cadera; ASTM F75; Prueba de Fatiga; Extensometría; ABNT NBR 7206-6:2013.

1. Introduction

Currently, technological advances have contributed to an enhancement in the quality of life. However, with the increase in life expectancy, new devices are necessary that more effectively meet human physical and biological needs (Bezerra,2017). Due to this increase in longevity, several illnesses, as well as trauma and fractures, can lead to the individual demands regarding the hip prosthesis uses. For example, total hip arthroplasty is a clinical condition that, if not detected early, can lead to joint problems since the youth (Guarnieiro,2010). Total hip prosthesis replacements are applied to patients affected by an accident or an illness of the CoCrMo hip (Savilahti,1997).

Hip prostheses have been used for more than 50 years due to their great properties, especially with regard to wear and corrosion resistances (Souza,2019). The procedure of replacing the joint with a prosthesis is called arthroplasty. Total Hip Arthroplasty (THA) is indicated when the conservative treatment fails and is understood as an effective procedure that provides better quality of life for patients, as it reduces pain and improves the functional capacity of the hip joint (Costa,2021). Nowadays, the standard treatment for degenerative joints is to replace them with medical devices, such as knee and hip prostheses, 70-80% of which are made of metallic biomaterials (Mckee,1966).

Most metallic biomaterial approaches are focused on stainless steels, cobalt-chromium alloys and titanium alloys, each of these materials has advantages and disadvantages (Silva Junior, 2021). Titanium alloys, for example, have a lower elastic modulus compared to stainless steel alloys and Co-Cr alloys, while reducing stress shielding (differences between responses to implant stiffness of human bone) (Geetha,2009).

Titanium implants suffer fatigue due to the cyclic mechanical loads provided by the contact parts that promote wear and friction, which lead to corrosion on the surface and consequently to a decrease in their fatigue resistance (Manivasagem, 2009). In turn, cobalt alloys exhibit high corrosion resistance and improved wear resistance (Niinomi,2012). The clinical use of these alloys for long time periods resulted in good compatibility in the mass form (Hanawa,2004). However, the corrosion-

assisted fatigue process has been reported to be the main failure mechanism of cobalt-chromium-molybdenum (CoCrMo) orthopedic devices (Hanawa,2002).

Fatigue is responsible for several failures in hip implants (Dias, 2021). Fatigue cracks are favoured as a function of stress concentrations after a certain number of cycles, and their propagation is accentuated due to the local brittleness (Silva, 2020). As the crack develops, there is a pronounced stress effects, resulting in an increase in the propagation speed of the crack and finally its propagation in its last stage when it reaches a critical size (Guesser, 2009). Often, the maximum tensile stresses on the stem and neck of a hip prosthesis are approximately 200 and 350 MPa, respectively (Chen,2015). The fatigue limit of implantable alloys depends on factors such as the manufacturing process and surface, microstructural, and fatigue conditions (Niinomi,2007). As examples of microstructural conditions, the content and types of inclusions and grain size are important aspects that influence in the lifespan of the prosthesis.

Throughout the walking process, the forces on the joint surface can vary from zero to several times the body weight (Paul, 1976). Contact areas also vary in complex ways, and typically they are on the order of several square centimeters (Atheshian, 1994). It is estimated that the maximum contact stresses on the hip can reach values of about 20 MPa during a step (Hodge, 1986). Orthopedic implants are subjected to static and / or cyclic efforts, most often of significant magnitudes. In view of these facts, it was necessary to characterize the durability and flaws of hip prostheses after performing the fatigue test. In Brazil, the Brazilian National Health Surveillance Agency – ANVISA – established modifications related to the minimum number of cycles to be supported by hip prostheses (old: 5,000,000 cycles; new: 10,000,000 cycles), according to the ABNT NBR 7206-6: 2013 standard.

In this context, the present work aims to validate the parts currently commercialized with the new standards, it being necessary to conduct tests to characterize the mechanical properties, with strain gauges that have linear response, which allow evaluating the strains on the prosthetic components. In this study, it was chosen by the method of linear electrical strain gauges.

No references were found in which the use of strain gauges to check the deformation of the prosthesis was applied to compare with the new Brazilian regulations. For this reason, this work presents an originality in relation to the analyzes often carried out in terms of strain values in hip prostheses.

This method goals to measure deformations of bodies by means of a strain gauge, when a material is subjected to the mechanical stresses, including tensile or compressive states. If an electric strain gauge with the appropriate characteristics is attached to the surface of the object, it corresponds a specific response of length according to the demands to which the surface is subjected (Matos,2020).

The use of strain gauges, despite being exposed to the high strain values, presents very small values of variation in electrical resistance; for this reason, it cannot be ideal for strain gauges to read this parameter directly. For this purpose, the numerous resources of the Wheatstone Bridge are placed (Geetha,2009). In addition, signal conditioners are used allied to strain gauges. Thus, the system can supply the excitation voltage to the Wheatstone bridge, and can amplify the signal received by it when the strain gauges deform, adapting the signal to the input characteristics of the measuring equipment.

2. Methodology

Specimens and three hot forged hip prostheses were used in this work, all of them composed by the Co-28Cr-6Mo alloy. The specimens consisted of prismatic pieces with 250 x 120 mm², and thickness values of 1.2 mm and 2.0 mm, respectively. Additionally, the prostheses were of the magnus type.

In summary, the following experimental tests were carried out to revalidate the Co-alloy according to the ANVISA: (a) chemical composition characterization (SEM/EDS analyses); (b) inclusion content and type, as well as grain size measurement, to compare with the limit described by the regulation (Optical microscopy - samples without and with metallographic etching, respectively); (c) tensile tests to assess mechanical properties of the alloy; and, finally, (d) fatigue tests to evaluate the number of cycles to be supported (stress and strain states) by the component, providing additional characterization especially of the possible cracks on the prosthesis surface. Specific descriptions of the adopted methodology are reported herein.

Applying scanning electron microscopy (SEM), data referred to the material chemical composition were collected by means of energy-dispersive X-ray spectroscopy (EDS) to verify the compliance with the ASTM F75 standard, conducting the semiquantitative chemical analysis of the alloy.

To perform the metallography tests, the samples were ground and polished with constant microstructural observation (optical microscope) to avoid the presence of scratches and oxidation, which could affect the analysis of the image and the data obtained from the microscopy. Afterwards, the inclusion content analysis was performed following the ABNT NBR NM 88 standard, considering the specimens without chemical etching.

The inclusion content determination was verified by comparing the specimen with standard images, corresponding to fields of view of 0.8 mm diameter and 100X magnification under the optical microscope. Following method 1 of the ABNT NBR NM 88 standard, five distinct regions of the sample at least should be compared to the images of nonmetallic inclusions of the Jernkontore type blade, taking into account their different levels, series, and types.

Generally, the presence of inclusions in metallic alloys contributes to the formation of brittle phases (non-metallic inclusions) during the steel manufacturing process, reducing the homogeneity of the material [19]. This can affect the useful life of the hip prosthesis, as well as fracture behavior during the displacement of the patient who has undergone the implant. In addition, small concentrations of inclusions provide better ductility, especially in surgical implants that are subjected to cold loading [20].

After the inclusion contents analysis, the chemical etching was performed following ASTM E407-07 - Standard Practice for Micro-Etching Metals and Alloys. According to this standard for alloys based on the cobalt element, it was defined to use the chemical etching number corresponding to 16 (5-10 ml HCl – 100 ml of deionized water - electrolytic at 3V immersed for 2 to 10 seconds in an area of 70 mm²).

Moreover, Heyn's intercept method (ABNT NBR 11568:2016) was used to measure the grain size considering the etched specimens analyzed using the optical microscopy. Because the grains tend to be equiaxial, for this method the line was drawn in a single plane of the specimen (C length in mm) to calculate the average length of the intercept (I). Equation 1 relates the grain quantities (A) to the average number of intercepts, N being designed as the magnification to obtain the grain size ABNT (TG).

$$I = \frac{C}{A \cdot N}$$

In which: I – Intercept average length, C – Line length, A- Quantity of grains; and N – 200X magnification.

Regarding the tensile tests, the procedures of the ABNT NBR ISO 6892-1: 2013 standard were followed, in which the specimens were subjected to the tensile force until the rupture of the material to determine mechanical properties based on the stress-strain curves, such as: elastic modulus, yield stress, tensile strength, elongation at break, among others.

Furthermore, fatigue tests were performed with three Co-28Cr-6Mo prostheses. The prostheses had no head incorporated into the nail for these tests, providing to be chosen according to the anatomy of the patient. The components were

positioned in a machined support fixed in the fatigue testing machine with surgical cement. Then, these prostheses were immersed in a physiological solution that simulates synovial fluid, which is often found in the joints, with a 0.9% NaCl solution composition, and was maintained using a heating system with electrical resistance and thermostat control at 37 ± 1 ° C.

For the fatigue test, a support was built with a metallic base attached to the equipment. This support presented an interchangeable acrylic body, where the fixing cement was inserted.

According to NBR 7206-6, the loads were applied at a specific point on the heads of the prostheses, whose position has been between 10° and 9° (included standard). To do this, the fixation and correct positioning were promoted by one piece developed with the 3D printing process, and the material applied was the PLA (polylactic acid) polymer.

After alignment with the support, the prosthesis was embedded in a supergrade structural cement with a compression strength of 50 MPa for 48 hours, replacing the 25 MPa strength, according to ABNT NBR 7206-6,

Another important step of the fatigue test preparation consisted of the solution flow that was possible by means of a aquarium pump connected from the support to the reservoir with 0.9% NaCl solution. Figure 1 displays the prosthesis prepared for the beginning of fatigue tests, with the container previously filled with saline solution, which allows simulating the synovial fluid.

Figure 1: Prosthesis submerged in 0.9% NaCl solution.



Source: Authors.

An apparatus was developed with an electronic system for capturing and processing information from extensometers installed in three main points in the prosthesis, based on the ABNT 7806-6: 2014 standard. This system was developed to promote the assessment of the prosthesis regions, which were more pronounced to suffer accentuated deformations. There is an upper part of the so-called prosthesis (neck), these points of the prosthesis that have the highest probability of failure with the development of cracks, and the function of the extensometers can be mapped focused on the conditions of strains on the material before, during, and after the crack propagation.

The project consisted of an assembly of the data acquisition circuit utilizing an instrumentation amplifier, in which the signal arising from the amplifier through the wheatstone bridge, and passed to the AD620 (low power instrumentation amplifier), as soon as the signal was handled by ADS1115 (analog-to-digital converter, Texas Instruments®). The programming was developed through the Arduino IDE using the Arduino Mega 2560 prototyping board.

Three sets of strain gauges with 10 channels were used for each model PA-06-031MF-120, which was made up of ten strain gauges that allowed variation of stress in relation to strain. The mapping was completed in the neck region of the component with sensors positioned at 30° , 45° and 90° of the reference extensometers.

The data acquisition circuit used the CI AD620, an instrumentation amplifier. The circuit presented $\frac{1}{4}$ of the Wheatstone bridge, of which, when the strain gauge was placed on the strain gauge connector, the bridge reproduced its proper functioning.

After fixing the prosthesis in the testing machine, the extensometers were connected in the developed case, data acquisition in their respective channels, being side A of channels related from 1 to 10, side B due to channels from 11 to 20, and side C corresponded to channels from 21 to 30.

To avoid reading errors, all strain gauges were calibrated at 0 volts and 0 Newton. The strain gauges have prone to contact the applied saline solution to simulate the body fluid. Furthermore, they must not present defects during the tests and, therefore, the cables were shielded to prevent short circuits. Thus, the prosthesis was subjected to the fatigue test with the 15 Hz cycle frequency at a maximum load of 2.5 kN, according to parameters defined in ABNT NBR 7206-4 regarding the fatigue tests in prostheses. The device performed 5 acquisitions of data per second, so that every 3 load cycles a reading was taken, generating an elastic deformation gradient in each reading axis.

Afterwards, the prosthesis was removed and a characterization was performed using penetrating liquid to verify the possible occurrence of cracks from the test. For the liquid penetrating test, the test specification parameters were based on the ASTM E-1417 and ASTM 165 standards.

3. Results and Discussion

The chemical composition of the studied Co-28Cr-6Mo alloy is revealed within the ASTM F75 standard according to Table 1, which denotes the average values resulting from the five different region analyses.

Table 1: Chemical composition measured in order to compare with the ASTM F75 specifications.

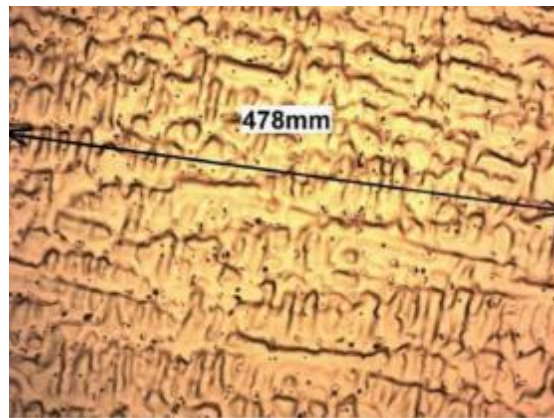
ELEMENT	MIN [%WT]	MAX [%WT]	AVERAGE VALUES [%WT]
Chromium	27	30	29.42
Molybdenum	5	7	6.71
Iron	---	0.5	0.07
Carbon	---	0.75	---
Silicon	---	0.35	0.25
Manganese	---	1.00	---
Tungsten	---	1.00	---
Phosphorous	---	0.20	0.04
Sulfur	---	0.020	---
Nitrogen	---	0.010	0.005
Aluminum	---	0.25	---
Titanium	---	0.10	---
Boron	---	0.010	---
Colbalt	balance	balance	53,7

Source: Authors.

As displayed in Table 1, the ASTM F75 standard establishes chromium levels between 27% and 30%, and molybdenum between 5% and 7%, with Cobalt in balance. The results presented remained within such limits in the regions without deviations. On the other hand, elements as silicon and carbon that could allow the material to become embrittled have been found insignificant values in view of the semi-quantitative approach.

The ABNT grain size of the material (TG) was estimated with respect to the Heyn intercept method, using an image with a 200X magnification obtained from an optical microscope. The test line was traced around 478 mm, according to the real scale, intercepting 21 grains, as shown in Figure 2, in which the average result was compared to other images.

Figure 2: Count of 21 grains presented along the test line, with a 200X magnification of optical microscope.



Source: Authors.

By replacing the measured values in Equation 1, the average length of the intercept resulting in:

$$I = \frac{C}{A \cdot N} = \frac{478 \text{ mm}}{21 \cdot 200} = 0.1138 \text{ mm}$$

According to the ABNT NBR 11568 standard, comparison with the average length value of the intercept with Table TG ABNT made it possible to identify that the grain size of the material was approximated to the number 3. To ensure appropriate control of the mechanical properties, the current standard implies that implants has been provided the grain size defined as number 5 or lower; therefore, the grains of the Co-28Cr-Mo prosthesis are within the required standards.

Furthermore, five regions were analyzed, based on the ABNT NBR NM 88: 2000 standard, which classifies material inclusions into four groups (sulfide, aluminate, silicate and globular oxides).

Only inclusions of the globular oxide group (type D) of the thin series were found in the optical micrographies of the five different regions, based on the specimens without metallographic etching and considering 1,000X magnification. These defects tend to have no influence on the biomaterial performance because they are in controlled amounts and morphologies, according to the Anvisa regulations. The same approach was conducted for higher magnifications using scanning electron microscopy (SEM), corroborating these results.

Moreover, round bars were applied to manufacture the specimens identified as CP1 and CP2 for the tensile tests. As previously commented, the values of mechanical properties obtained were compared with the minimum standards included by ASTM F75.

The graphs generated by the software from which the test data were collected in real time. The yield limit was determined in a more commonly used mode, drawing a straight line parallel to the elastic region with a deformation of 0.002 until crossing the stress-strain curve. The mechanical properties for CP1 and CP2 are provided in Table 2. The comparison between the experimental results and the ASTM F75 standard allowed identifying that the samples slightly pointed out lower properties, which can affect the fatigue results that consists of the main object of this study.

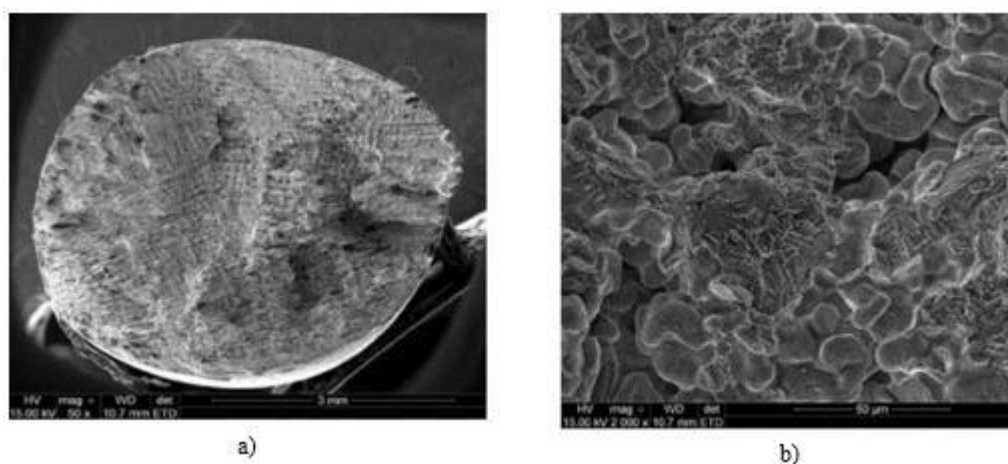
Table 2: Results obtained from the tensile tests – mechanical properties of the alloy studied.

	ELASTIC MODULUS [GPA]	YIELD STRESS [MPA]	ULTIMATE TENSILE STRENGTH [MPA]	STRESS AT BREAK [MPA]	ELONGATION [%]
CP 1	47.37 ± 0.22	262.3	626.2	559.5	6.2
CP 2	48.91 ± 0.20	193.9	550.1	537.5	7.4
ASTM F75	---	450	655	---	8.0

Source: Authors.

Fracture characterizations using SEM of one of the specimens submitted to the tensile tests (CP1) were also analyzed. It was possible to verify planimetric portions that indicated a reduced ductility of the material, as shown in Figures 3.

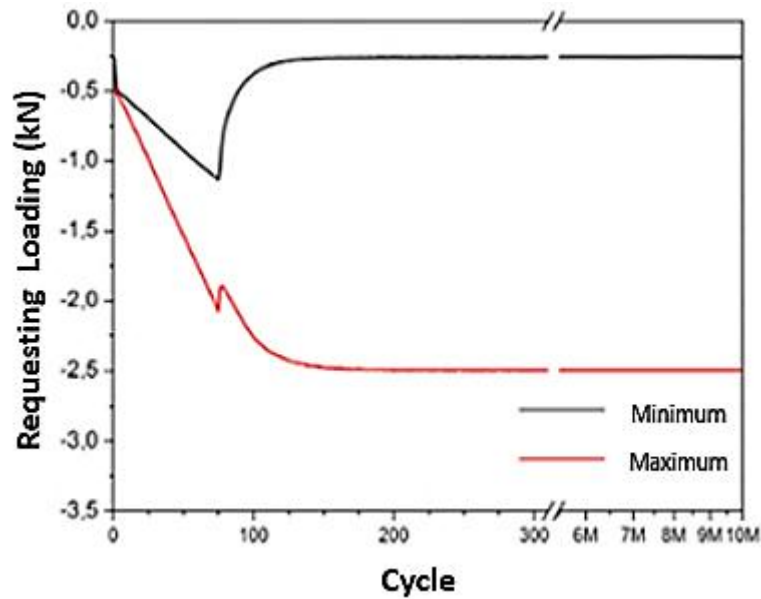
Figure 3: a) SEM image of the fracture (overview) of CP1 after the tensile test and b) Grains surface modified by breaking the material (after the CP1 tensile test of the CP1) – secondary electron image by SEM.



Source: Authors.

In fatigue tests, the prosthesis was subjected to 10,450,000 cycles with an applied load of 2.5 kN in two phases: the first phase with 2,000,000, and the second one with 8,450,000. In the post-test analysis it was found that the prosthesis did not present any deviation after applying the load, that is, the component did not present plastic deformations, fracture, or oxidation. Figure 4 shows a graphic representation of the load applied as a function of the number of cycles of the test. It can be observed that the equipment, at the beginning of the test, was self-regulating to reach the maximum limit established corresponding to a load of -2.5 kN as parameters of the NBR 7206-4 standard. Approximately 100 cycles of 15 Hz were necessary to reach the stipulated load and remain stable in this load until the end of the fatigue test at 10.4 million cycles.

Figure 4: Graphical maximum and minimum load ratios, obtained from the fatigue test equipment of an Instron machine.

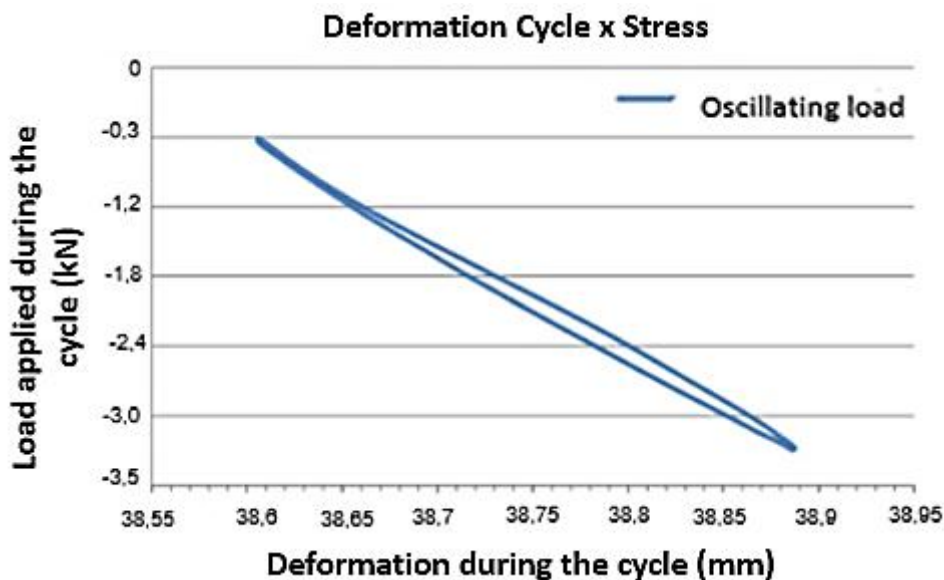


Source: Authors.

Analyzing the stress x strain graph at the beginning of the test in 1 million cycles and at the end of the test with 10.4 million cycles (Figure 5), it was found that the deformation remained constant at 0.3 mm throughout the material fatigue test.

After the prosthesis was instrumented with the extensometers, an electronic system was developed. This system performs the reading and processing of the data from the fatigue test of the prosthesis with extensometry and is equipped with an electronic circuit. With the prosthesis attached to the fatigue testing machine, the extensometers were connected to the data acquisition case.

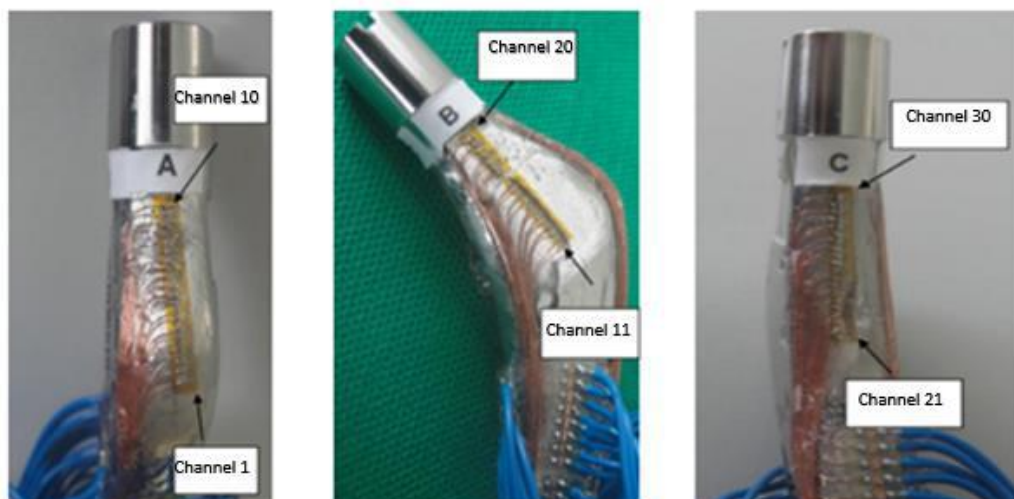
Figure 5: Deformation graph repeated throughout the 10.4 million cycles.



Source: Authors.

The positions to detect individual strain and stress variations of the A, B and C axes, which represent the 3 sides of the neck of the local prosthesis, where the data analysis was performed, are represented in Figure 6. The images are provided to detail the area of the greatest risk of fracture using data striped in axes reported in NBR 7206-4.

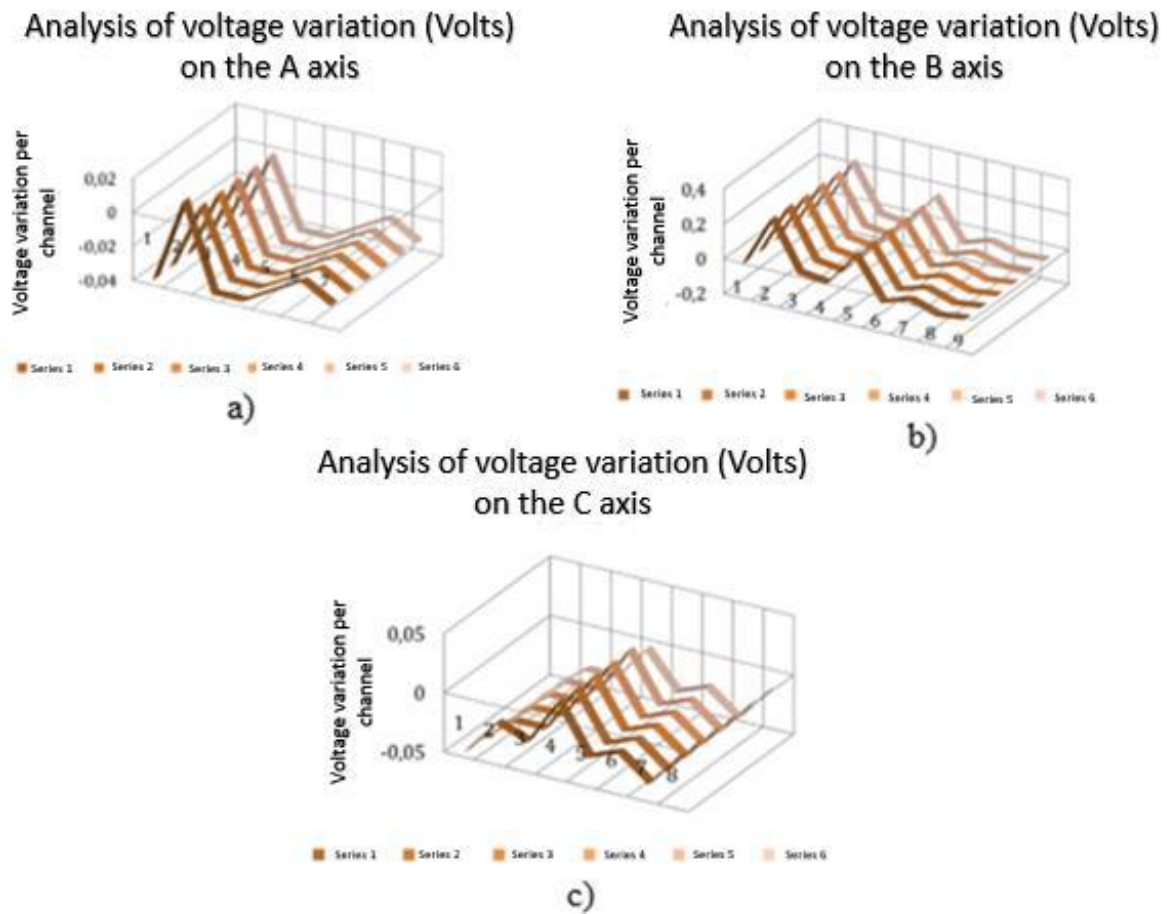
Figure 6: Prostheses with extensometers fixed on their A, B, and C axes.



Source: Authors.

Figure 7 shows the values arising from the reading of the electrical voltage based on the load applied to the prosthesis submitted to the fatigue test with extensometry; therefore, it made it possible to verify specific places in the prosthesis that suffered more pronounced elastic deformations.

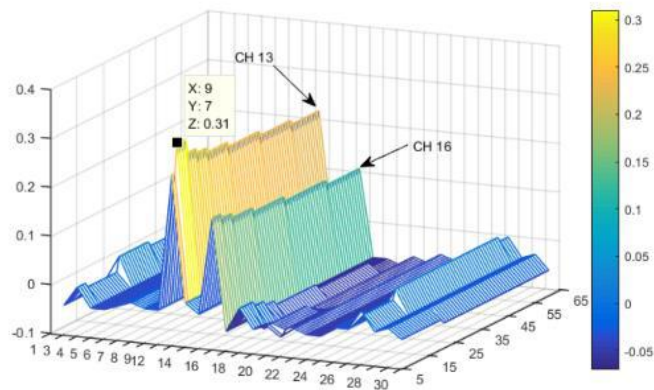
Figure 7: Graph of the acquisition of extensometry data: a) on the A axis of the prosthesis, b) on the B axis of the prosthesis, and c) on the C axis of the prosthesis.



Source: Authors.

Additionally, Figure 8 points out the behavior of the electrical voltage due to all extensometers attached to the prosthesis, indicating the relation between the applied load and variation of electrical voltage, made it possible to obtain a deformation gradient in relation to the applied load.

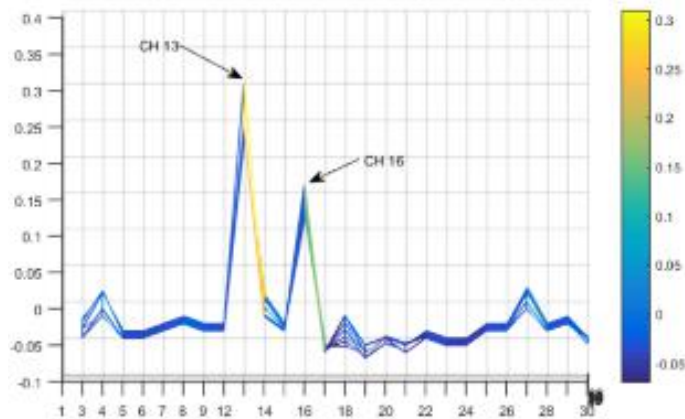
Figure 8: Voltage variation of the extensometers as a function of the 2.5 kN load.



Source: Authors.

Analyzing Figures 9 and 10, it can be possible to verify and identify the points where the prosthesis suffered the higher elastic deformation, making it evident points of channels 13 and 16, located on the B axis of the prosthesis, and thus indicating the points where the prosthesis undergoes more deformation.

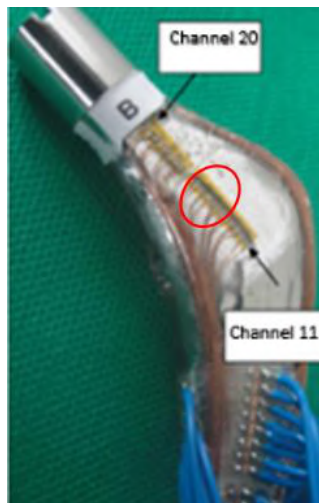
Figure 9: Details of the highest and lowest voltage levels per channel.



Source: Authors.

The regions of channels 13 and 16 were located in the neck of the prosthesis, in which this region was subjected to greater deformation, depending on the applied moments. This region can be seen in depth in Figure 10.

Figure 10: Details of the highest and lowest voltage levels per channel.



Source: Authors.

After the fatigue test and subsequent visual inspection of the prosthesis being submitted to all the steps determined by the ASTM E-1417 and ASTM 165 standards, the analysis by liquid penetrant inspection allowed to confirm that no macrocracks were found on the surface of the component. To conclude, as determined by the ASTM E-1417 and ASTM 165 standards, regarding the revelation of cracks by application of liquid penetrant inspection, no cracks were found in the prosthesis.

4. Conclusion

After the experimental tests, the Co-28Cr-6Mo alloy was revalidated to meet the ANVISA new regulations applied to the hip prosthesis. Several parameters have been evaluated concerning fatigue and tensile tests, and grain size and inclusion studies. It was possible to verify that the prostheses withstood the test of 10.4 million cycles with a minimum load of 0.25 kN, and a maximum load of 2.5 kN, both in compression, without showing evidence of cracks or surface fractures. The extensometry signal acquisition device captured the deformations suffered by the prostheses, allowing a control of the deformation gradient of the prosthetic neck region. Only elastic deformations were found to occur in the material. When analyzing the stress x strain graphs in 1 million cycles (at the beginning of the test), and with 10.4 million cycles (at the end of the test), it was found that the deformation remained constant at 0.3 mm throughout the fatigue tests. Furthermore, when analyzing the extensometry data were analyzed, it was possible to observe the variation of the acquisition voltage per channel in relation to the cyclic load applied to the fatigue test. Based on this evaluation, it is possible to affirm that each strain gauge on the A, B or C axis suffered elastic deformations, considering the maximum load applied of 2.5 kN. The grain size of the material was about number 3, in which the ABNT NBR 15628-3 standard emphasizes that the average grain size of the material must be number 5 or less. The inclusion content, based on the ABNT NM 88 - Method 1 standard using five regions analyzed, was only found the Type D of the thin series (globular oxides), with quantities and morphology allowed by the standard. Finally, the thermal treatment performed by solubilization could be conducted in order to minimize the presence of inclusions, and thus, with insertion in a patient, this action should reduce the effect caused by synovial fluid. Nonetheless, the prosthesis withstood the application of ten million cycles without showing surface cracks at depths up to 10 mm, which enables its applications.

In future works, we suggest the use of extensometry for the analysis of failures in prostheses and screws with a large number of uses and in implant surgeries. In addition to improving the data acquisition system for other types of sensors and creating a wireless communication system (bluetooth, wi-fi) storing the information in the cloud.

Acknowledgments

The authors are very grateful to CNPq (National Council for Scientific and Technological Development), for the scholarship and financial assistance, which allow full dedication within the Universidade Presbiteriana Mackenzie graduate program and operationalization of the study.

References

- Ateshian, G. A. (1994). A stereophotogrammetric method for determining in situ contact areas in diarthrodial joints, and a comparison with other methods. *Journal of Biomechanics*, 27(1), 111–124. [https://doi.org/10.1016/0021-9290\(94\)90038-8](https://doi.org/10.1016/0021-9290(94)90038-8)
- Bezerra, E. (2017). Avaliação de não conformidades de próteses de quadril fabricadas com ligas de titânio e aço inox. *Matéria* (Rio de Janeiro), 22(1). <https://doi.org/10.1590/s1517-707620170001.0114>
- Chen, Q., & Thouas, G. A. (2015). Metallic implant biomaterials. *Materials Science & Engineering. R, Reports: A Review Journal*, 87, 1–57. <https://doi.org/10.1016/j.mser.2014.10.001>
- Costa, L. dos S. (2021). Hip arthroplasty: Effective rehabilitation protocols. *Research, Society and Development*, 10(4), e45510414370. <https://doi.org/10.33448/rsd-v10i4.14370>
- Dias, D. F., & Gonçalves, S. J. da C. (2021). Falhas em implantes de quadril. *Research, Society and Development*, 10(11), e357101119668. <https://doi.org/10.33448/rsd-v10i11.19668>
- Geetha, M. (2009). Ti based biomaterials, the ultimate choice for orthopaedic implants – A review. *Progress in Materials Science*, 54(3), 397–425. <https://doi.org/10.1016/j.pmatsci.2008.06.004>
- Guarniero, R. (2010). Displasia do desenvolvimento do quadril: atualização. *Revista Brasileira de Ortopedia*, 45(2), 116–121. <https://doi.org/10.1590/s0102-36162010000200002>

- Guesser, W. L. (2009). Propriedades mecânicas dos ferro fundidos, Issuu. https://issuu.com/editorablucher/docs/issuu_ferros_fundidos_isbn9788521205012.
- Hanawa, T. (2002). Evaluation techniques of metallic biomaterials in vitro. *Science and Technology of Advanced Materials*, 3(4), 289–295. [https://doi.org/10.1016/s1468-6996\(02\)00028-1](https://doi.org/10.1016/s1468-6996(02)00028-1)
- Hanawa, T. (2004). Metal ion release from metal implants. *Materials Science & Engineering. C, Materials for Biological Applications*, 24(6–8), 745–752. <https://doi.org/10.1016/j.msec.2004.08.018>
- Hodge, W. A. (1986). Contact pressures in the human hip joint measured in vivo. *Proceedings of the National Academy of Sciences of the United States of America*, 83(9), 2879–2883. <https://doi.org/10.1073/pnas.83.9.2879>
- Manivasagam, G. (2010). Biomedical Implants: Corrosion and its Prevention - A Review. *Corrosion Science*, 2, 40–54.
- Matos, D. B. (2020). Instrumentação de um sistema de sensoriamento: montagem de uma plataforma protótipo para a aquisição do empuxo de propulsores eletromecânicos / instrumentation of a sensing system: assembly of a prototype platform for the purchase of electromechanical propellers. *Brazilian Journal of Development*, 6(10), 78039–78050. <https://doi.org/10.34117/bjdv6n10-290>
- McKee, G. K., & Watson-Farrar, J. (1966). Replacement of arthritic hips by the McKee-Farrar prosthesis. *The Journal of Bone and Joint Surgery*. British Volume, 48(2), 245–259. <https://pubmed.ncbi.nlm.nih.gov/5937593/>
- Niinomi, M. (2007). Fatigue characteristics of metallic biomaterials. *International Journal of Fatigue*, 29(6), 992–1000. <https://doi.org/10.1016/j.ijfatigue.2006.09.021>
- Niinomi, M. (2012). Development of new metallic alloys for biomedical applications. *Acta Biomaterialia*, 8(11), 3888–3903. <https://doi.org/10.1016/j.actbio.2012.06.037>
- Paul, J. P. (1976). Force actions transmitted by joints in the human body. *Proceedings of the Royal Society of London. Series B, Containing Papers of a Biological Character*. *Royal Society (Great Britain)*, 192(1107), 163–172. <https://doi.org/10.1098/rspb.1976.0004>
- Savilahti, S. (1997). Survival of Lubinus straight (IP) and curved (SP) total hip prostheses in 543 patients after 4–13 years. *Archives of Orthopaedic and Trauma Surgery*, 116(1–2), 10–13. <https://doi.org/10.1007/bf00434092>
- Silva, C. G. I. da, & Gemelli, E. (2020). Influência da corrosão e de tensões cíclicas alternadas na vida em fadiga dos ferros fundidos nodulares das classes FE 50010 e FE 50007. *Matéria (Rio de Janeiro)*, 25(2). <https://doi.org/10.1590/s1517-707620200002.1024>
- Silva Junior, W. C. (2021). Obtaining the predicted number of cycles of femoral prosthesis manufactured with ASTM F138 and ASTM F75 alloys, applying the method of finite element. *Journal of Physics. Conference Series*, 1730(1), 012026. <https://doi.org/10.1088/1742-6596/1730/1/012026>
- Souza, C. M. P., & Silva Junior, W. C. (2019). Comparação de desempenho da prótese de quadril fabricadas nos materiais ASTM F75, F136 e F138. <https://doi.org/10.5281/ZENODO.3460918>